Clinical Research Report

Journal of INTERNATIONAL MEDICAL RESEARCH

Journal of International Medical Research
2019, Vol. 47(4) 1555–1564

DOI: 10.1177/0300060518823630
journals.sagepub.com/home/imr
SAGE

Stress distribution in a mandibular premolar after separated nickel-titanium instrument removal and root canal preparation: a three-dimensional finite element analysis

Na Ni[1,2], Jing Ye[1], Liyuan Wang[2], Simin Shen[2], Lei Han[3] and Yuxia Wang[2]

Abstract

Objective: This study used finite element analysis (FEA) to assess the von Mises stresses of a mandibular first premolar after removing a separated instrument with an ultrasonic technique.

Methods: FEA models of the original and treated mandibular first premolar were reconstructed, and three models (the original canal, size 30/taper 0.04 canal, and separated instrument removal canal) were created. Two-direction (vertical and lateral) loading patterns were simulated with a 175-N force. The maximum von Mises stresses of the models within the roots from the apex to the cervical region were collected and summarized.

Results: Under vertical and lateral loads, all maximal values in the three models were localized in the straight-line access region. Compared with the original model (model 1), the treated models (models 2 and 3) had greater maximum stress values from the apex to the cervical region. Greater differences in the maximum von Mises stresses between models 2 and 3 were present in the straight-line access region.

Conclusions: Separated instrument removal caused changes in stress distribution and increases in stress concentration in the straight-line access region of roots.

[1]Department of Stomatology, Tianjin Hospital, Hexi District, Tianjin, China
[2]Department of Endodontics, Tianjin Stomatological Hospital, Heping District, Tianjin, China
[3]Department of Radiology, Tianjin Stomatological Hospital, Heping District, Tianjin, China

Corresponding author:
Na Ni, Department of Stomatology, Tianjin Hospital, 406 Jiefangnan Road, Hexi District, Tianjin 300211, China.
Email: nina_tjskq@163.com

Keywords
Finite element analysis, stress distribution, von Mises stress, loading patterns, separated instrument, ultrasonic technique, cone-beam computed tomography, mandibular premolar

Date received: 10 July 2018; accepted: 17 December 2018

Introduction

Instrument fracture inside the root canal is a serious problem during endodontic treatment.[1] Broken endodontic instruments may block access to the apical constriction, thereby hindering the efficacy of root canal shaping and cleaning, and impacting root canal therapy outcomes.[2] Separated instrument fragments may originate from stainless steel (SS), nickel-titanium (NiTi), and carbon steel instruments.[3,4] The known fracture rate of NiTi instruments is 0.4% to 10%, while that of SS instruments is 0.25% to 7.4%.[4–7]

Orthograde and surgical approaches are commonly used to manage separated instruments. An orthograde approach is performed to remove separated instruments, bypass separated instruments, or clean, shape, and fill around fragments.[2] Notably, the first choice is retrieval from the root canal.[8] However, there are no standardized management approaches to ensure successful fragment removal.[9] Ruddle et al.[10] introduced a technique for fragment removal that involves the use of modified Gates-Glidden burs, ultrasonic devices, and a dental operating microscope.

Removal of bulk dentin during endodontic treatment is known to weaken the mechanical strength of teeth.[11] However, structural dentin changes that affect stress distribution on the tooth root are unknown. Stress distributions are generally utilized to predict tooth fracture because a concentration of stress indicates a region of potential fracture.[12] Finite element analysis (FEA) is a powerful method that can be combined with numerical simulation to develop a quantitative numerical model for evaluating stress distributions and magnitudes in teeth.[13,14] A cone-beam computed tomography (CBCT) image of the tooth provides three-dimensional (3D) anatomic structural information for an FEA model. Then, an FEA approach creates a digital model of the tooth, model loads, and boundary conditions in a virtual environment. Thus far, studies have primarily used FEA combined with mathematical tooth modeling algorithms to describe stress distributions in endodontically treated teeth (ETT),[15,16] but there have been no evaluations of stress distributions in the root after completely removing separated instruments from the root canal with an FEA approach.

Therefore, in this study, an FEA approach was used to evaluate the maximum von Mises stresses from the apex to the cervical region of a mandibular first premolar after removing a separated instrument by using an ultrasonic technique under a dental operating microscope.

Methods

A mandibular permanent first premolar, extracted because of severe periodontal bone resorption, was collected in accordance with the following criteria: (1) it had completely formed roots; (2) it had no carious cavities, root resorption, root canal treatment, or restoration; and (3) it had no root fracture or crack in the surface of the root, when observed under a dental operating microscope (Opmi Pico, Carl Zeiss, Oberkochen, Germany). The treatment plan and reasons for collection of the tooth were explained to

the patient, and appropriate informed consent was obtained. The Institutional Review Board of Tianjin Hospital, Tianjin, China approved this study (Approval No. 2018029).

Fractured NiTi endodontic instrument model generation

After preparing the access cavity and removing pulp debris, a preoperative radiograph of the mandibular first premolar was recorded using a CBCT system (J. Morita Mfg. Corp., Kyoto, Japan) operated at 80 kVp and 5 mA, with a scanning time of 9.4 s and slice thickness of 0.125 mm. Image acquisition was performed by an experienced oral radiologist, in accordance with the manufacturer's instructions (Figure 1a). Root canal preparation was performed using Mtwo® files (VDW, Munich, Germany) with a crown-down technique. To create a separated NiTi fragment within the root canal, a #25/0.06 taper Mtwo® file was used; this file was notched to a depth of half of the instrument thickness at a 4-mm distance. The separated instrument model was generated by controlling the speed and torque of rotation.

Fractured NiTi endodontic instrument removal procedure

The following sequence of steps was used to remove the separated instrument. First, a CBCT image was taken to confirm the location of the fractured instrument fragment. In Figure 1b, the fragment is located 4 mm from the apical foramen. In this study, fractured instrument removal was performed by one endodontic specialist. Modified Gates-Glidden burs were used to prepare a staging platform at the level of the fragment, thus allowing the separated instrument and surrounding dentin to be observed under a dental operating microscope. The ultrasonic device was then set to medium power (29 kHz) to avoid fracturing the ultrasonic tip. An ET25 ultrasonic tip (Satelec, Bordeaux, France) was applied in a counterclockwise direction. Ultrasound vibrations were transmitted to the fragment, which caused loosening and dislodging, such that the fragment could eventually be removed. Finally, a CBCT image (treated image) was taken to confirm fragment retrieval (Figure 1c).

3D FEA models generation

The FEA model was the basis for the model analysis (Figure 2a). First, images (original and treated images) of each layer were imported into Mimics software (Mimics, V17.0, Materialise, Belgium) and edited to create closed contours based on the gray-scale levels of enamel, dentin, and pulp. These contours in different layers were

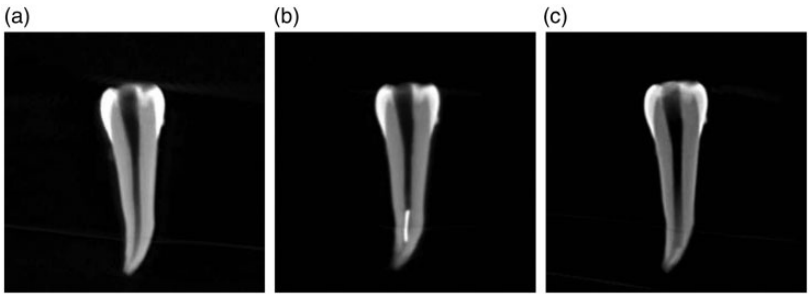

Figure 1. Cone-beam computed tomography images. (a) Preoperative radiograph of the mandibular first premolar; (b) Radiograph of a fractured NiTi endodontic instrument in the root canal; and (c) Postoperative radiograph of the mandibular first premolar

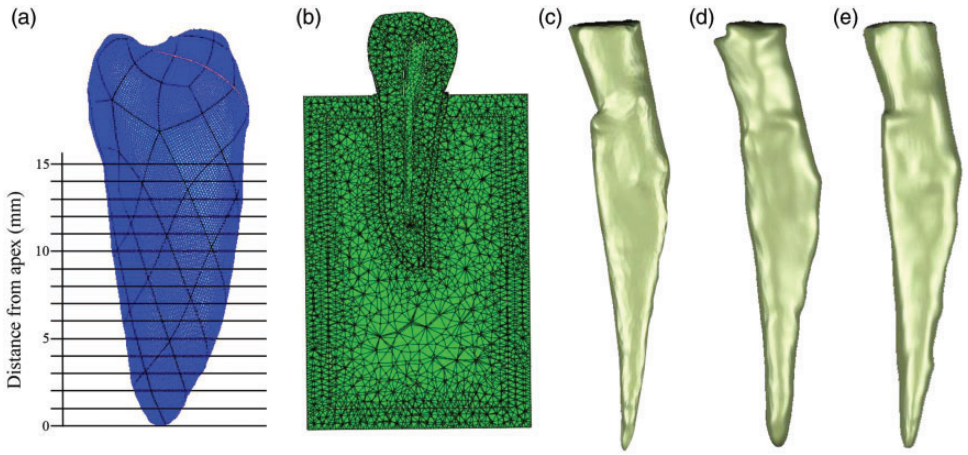

Figure 2. Three-dimensional finite element analyses models. (a) Finite element model of the mandibular premolar. (b) Model of sagittal plane. Three simulated root canals are shown: (c) the original canal (model 1); (d) the size 30, taper 0.04 canal (model 2); and (e) the separated instrument removal canal (model 3)

used to reconstruct 3D surface models of the original and treated mandibular first premolars. The 3D surface models (original and treated models) were then imported into the Geomagic Studio software (Geomagic Studio, V12.0, Raindrop Geomagic, Rock Hill, SC, USA) to obtain the NonUniform Rational B-Splines of the models. The original model (model 1) was designated as the control, and model 2 was created from model 1 after simulating root canal preparation (size 30, taper 0.04). The treated model was reconstructed as the control, and model 3 was created after simulating root canal preparation (size 30, taper 0.04) (Figure 2). Supporting structures (length: 25 mm, width: 20 mm, and height: 30 mm), including periodontal ligament (PDL) (thickness, 0.2 mm), cortical bone (thickness, 2 mm), and cancellous bone, were modeled around the tooth root, as shown in Figure 2b. Finally, all models were meshed by Hypermesh software (Hypermesh, V13.0, Altair, Troy, MI, USA). The element sizes of the three models and supporting structures were 0.5 mm and 1.0 mm, respectively. All surface contacts were assumed to represent complete bonding without relative movement. The numbers of nodes and elements for the dentin in each model are shown in Table 1.

Table 1. Numbers of nodes and elements of dentin for each model

	Number of nodes	Number of elements
Model 1	3620	15076
Model 2	4376	18543
Model 3	4188	17522

Boundary conditions and model loads

The mesial (M) and distal (D) surfaces of the alveolar bone were constrained in six degrees of freedom. Two-direction (vertical and lateral) loading patterns were simulated with a 175-N force and applied to two 1-mm^2 areas.[17,18] The lateral load was applied to the lingual plane of the cusp at a 45° angle to the longitudinal axis of the mandibular premolar. Each part of the whole model was imported into the Abaqus software (Abaqus, V6.14, Dassault Simulia, Johnston, RI, USA) to perform static

linear analysis. Different simulated material properties (Young's modulus (E) and Poisson's ratio values) were generated, based on data from the literature (Table 2).[15,17,19] Cross-sections of root canal were created from the apex at intervals of 1.0 mm. To visualize the stress distributions and magnitudes in the models, the data were transformed into color graphics. The maximum von Mises stresses within the roots of the models, from the apexes to the cervical regions, were collected and summarized. The root was divided into three regions as follows: straight-line access region (9–15 mm from the apex), separated instrument region (5–8 mm from the apex), and apical region (1–4 mm from the apex).

Table 2. Simulated material properties

Material	Young's modulus (GPa)	Poisson's ratio	Reference
Enamel	84.1	0.33	15,19
Dentin	18.6	0.31	17,19
Periodontal ligament	0.0689	0.45	15
Cortical bone	13.7	0.30	17
Trabecular bone	1.37	0.30	15

Results

Bidirectional (vertical and lateral) occlusal loads were applied to the three models; the resulting stress distributions differed among the models. Figures 3a–c and Figures 4a–c show the 3D stress distributions from the apex to the crown. Figures 3d–f and Figures 4d–f show the stress distributions in the axial plane in the straight-line access regions (9–15 mm from the apex). The maximum von Mises stresses under a vertical load, from the apexes to the cervical regions, are shown in Table 3; those under a lateral load are shown in Table 4.

Under a vertical load, the maximal values of models 1, 2, and 3 were 10.475 MPa

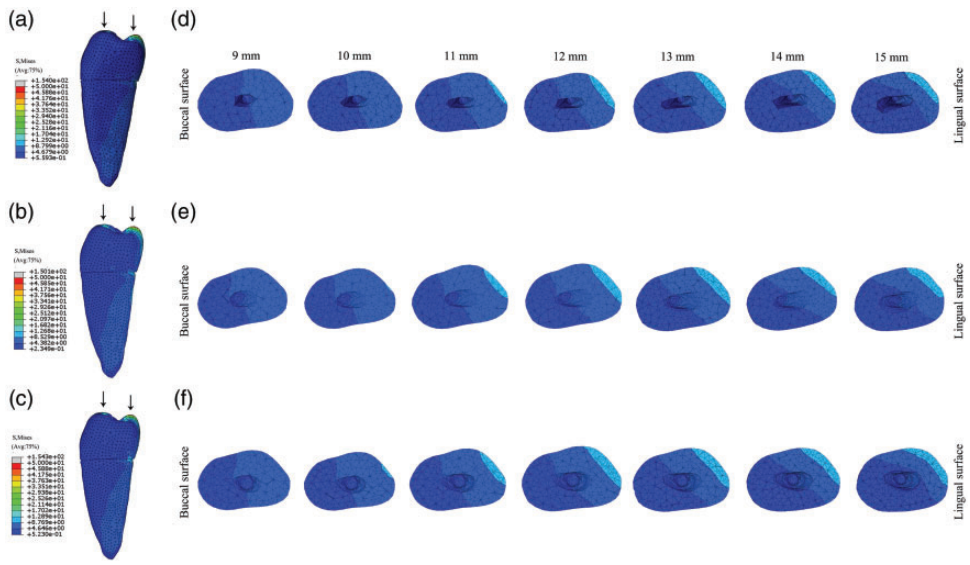

Figure 3. Finite element analyses of the original and treated models under vertical loading. (a–c) Three-dimensional stress distributions in models 1, 2, and 3, respectively. (d–f) Stress distributions in the axial plane in the straight-line access regions (9–15 mm from the apex) of models 1, 2, and 3, respectively

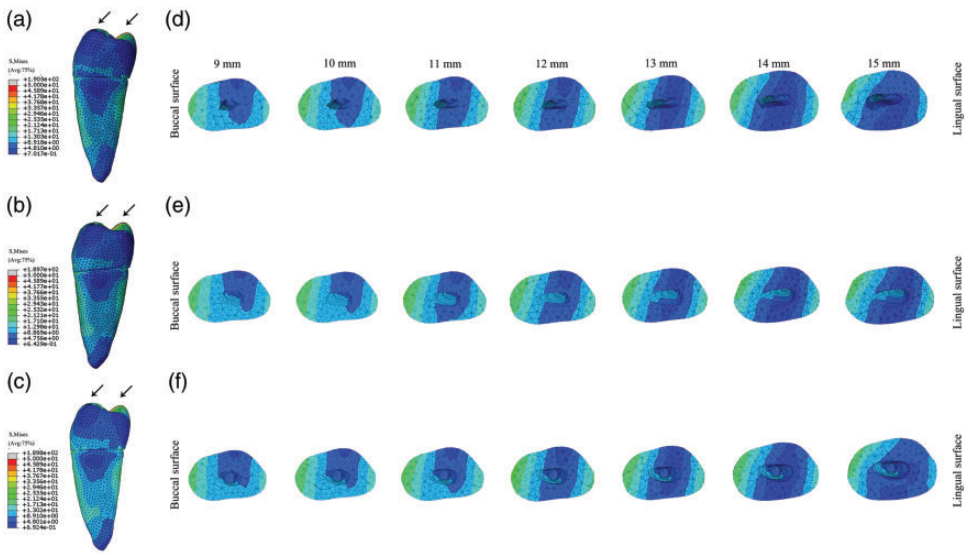

Figure 4. Finite element analyses of the original and treated models under lateral loading. (a–c) Three-dimensional stress distributions of models 1, 2, and 3, respectively. (d–f) Stress distributions in the axial plane in the straight-line access regions (9–15 mm from the apex) of models 1, 2, and 3, respectively

(in the 13-mm region), 10.949 MPa (in the 15-mm region), and 11.346 MPa (in the 15-mm region), respectively. The maximal values in the three models were all in the lingual surface of the straight-line access region. Model 2 (size 30, taper 0.04 canal) and model 3 (separated instrument removal canal) had greater maximum stress values than did model 1 (original canal) from the apex to the cervical region. Model 3 had greater stress values than model 2, except in the 1-mm and 4-6-mm regions. In model 3, the difference was more distinct, particularly in the 10-mm region; the stress value was 1.101 MPa greater in model 3 than in model 2 (Table 3).

Under a lateral load, the maximal values of models 1, 2, and 3 were 22.378 MPa, 24.147 MPa, and 24.842 MPa, respectively. Additionally, the maximal values of the models were all in the buccal surface of the 12-mm region. Moreover, the maximal values of all three models were observed in the straight-line access region. The differences between model 1 and each of the other models were similar to those of the vertical load in these models. Model 3 had greater stress values than model 2, except in the 1-mm region. In model 3, the difference was more distinct, particularly in the 11-mm region; the stress value was 1.045 MPa greater in model 3 than in model 2 (Table 4).

Discussion

Successful removal of a separated instrument from a root canal system is a challenging and time-consuming procedure. Among the devices and techniques that are available for the removal of a separated instrument, ultrasonic devices and the dental operating microscope have become increasingly important.[9] In a study of 24 patients, Ward et al.[20] reported a success rate of 66.6% for removing a separated instrument with an ultrasonic technique. Shahabinejad et al.[9] achieved an 80% success rate in removing fragments with an ultrasonic technique. In the clinical setting, a staging

Table 3. Maximum von Mises stresses within roots under vertical load (MPa)

	Model 1 Original canal	Model 2 Size 30 taper 0.04 canal	Model 3 Separated instrument removal canal
1 mm	4.488	5.957	5.923
2 mm	4.984	4.971	4.983
3 mm	6.093	6.295	6.796
4 mm	7.345	7.809	7.697
5 mm	8.065	8.467	8.265
6 mm	8.050	8.276	8.174
7 mm	7.998	8.107	8.343
8 mm	7.936	7.990	8.473
9 mm	8.171	8.250	8.399
10 mm	8.806	8.988	9.351
11 mm	9.510	9.525	9.899
12 mm	9.923	10.230	10.488
13 mm	10.475	10.701	10.945
14 mm	10.141	10.688	10.830
15 mm	10.230	10.949	11.346

Table 4. Maximum von Mises stresses within roots under lateral load (MPa)

	Model 1 Original canal	Model 2 Size 30 taper 0.04 canal	Model 3 Separated instrument removal canal
1 mm	6.411	6.899	6.793
2 mm	10.722	11.266	11.566
3 mm	12.581	12.775	12.919
4 mm	13.102	13.308	13.803
5 mm	13.668	13.759	13.939
6 mm	15.462	15.996	16.374
7 mm	16.910	17.284	17.791
8 mm	18.857	19.002	19.015
9 mm	19.897	20.400	20.470
10 mm	21.264	21.937	22.508
11 mm	21.907	22.153	23.198
12 mm	22.378	24.147	24.842
13 mm	20.044	20.873	21.428
14 mm	22.063	22.211	22.955
15 mm	22.278	24.113	24.313

platform prepared by using a modified Gates-Glidden bur should remain centered to ensure optimal visualization of the fractured file and minimize the risk of root perforation. Fine ultrasonic tips of different sizes and lengths are now manufactured for use in patients with different characteristics, in order to increase the success rate of separated instrument removal. Ideally, the fractured instrument should be successfully

removed from the root canal while incurring minimal damage to surrounding tissues.

However, after retrieval of a fragment from the root canal, the affected tooth exhibits a risk of root fracture because enlargement of the root canal is unavoidable during this procedure. Notably, ETT are more likely to experience vertical root fractures.[21] The prognosis of tooth root fracture is poor; eventually, the tooth may be lost and require extraction.[22] Chen et al.[22] demonstrated that removal of bulk dentin from the root canal changed stress distribution in the root. Tang et al.[23] also reported that multiple factors, including root anatomy, canal shape, and dentin thickness, can affect stress distribution in the root during occlusal loading. Stress distribution within the root is an important indicator related to the prognosis of ETT.[12] Excessive force can lead to crack formation within the root canal in areas that experience concentrated stress.[24] These results are consistent with the conclusions of the present study: under both vertical and lateral loads, the treated models (models 2 and 3) had greater maximum stress values from the apex to the cervical region, compared with the original model (model 1).

Good access and visualization are known to play important roles in ensuring the successful and safe retrieval of fragments.[20] Thus, clinicians must remove dentin to create straight-line access to the fragment. In the present study, under vertical and lateral loads, all maximal values in models 2 and 3 were located in the straight-line access regions. Additionally, the greatest differences between models 2 and 3 appeared in the straight-line access regions (the 10-mm and 11-mm regions), which suggests that excessive removal of the dentin structure to create straight-line access increases stress values, thereby increasing the risk of crack formation. Ultrasonic devices and the dental operating microscope play important roles in ensuring the success of fragment removal and minimizing the unnecessary removal of bulk dentin during treatment. A dental operating microscope permits direct visualization to locate fragments and allows the clinician to remain centered within the root canals.[8]

With the development of digital imaging techniques, more efficient methods have been used to obtain anatomical models. In CBCT imaging, serial sagittal, coronal, and axial views allow excellent visualization of root canal anatomy with a low dosage of radiation. Thus, CBCT is recommended as a useful tool in endodontics for the evaluation of separated instruments; this approach supports treatment planning and outcomes.[25,26]

An FEA is one of the most successful approaches to evaluate stress distributions in complex teeth and resolve treatment challenges.[27] The accuracy of the FEA method depends on the availability of complete comprehensive models, which include the whole-tooth structure and supporting structures, in order to evaluate tooth strength and root fracture risk. However, some limitations must be considered in these particular FEA studies; these include the particular tooth morphology, tooth structure, supporting structures, magnitude of loads, direction of loads, and material properties that were used in the present study, which may not be applicable to other studies that use different parameters. Because a single condition or a few conditions were evaluated for each of these parameters, the results from this study cannot be completely applied to other teeth or other loading conditions. Additional models of other teeth under different loading conditions should be studied to evaluate stress distributions in the root after removal of a separated instrument.

In conclusion, the treated models (size 30, taper 0.04 canal; and separated instrument

removal canal) showed greater maximum stress values than the original model (original canal), from the apexes to the cervical regions. Greater differences in the maximum von Mises stresses between models 2 and 3 were localized in the straight-line access regions under vertical and lateral loads. Separated instrument removal caused changes in stress distribution and increases in stress concentration in the straight-line access region of roots.

Declaration of conflicting interest

The authors declare that there is no conflict of interest.

Funding

This research received no specific grant from any funding agency in the public, commercial, or not-for-profit sectors.

ORCID iD

Na Ni http://orcid.org/0000-0001-6385-0828

References

1. Parashos P and Messer HH. Rotary NiTi instrument fracture and its consequences. *J Endod* 2006; 32: 1031–1043.
2. Madarati AA, Hunter MJ and Dummer PM. Management of intracanal separated instruments. *J Endod* 2013; 39: 569–581.
3. Ankrum MT, Hartwell GR and Truitt JE. K3 Endo, ProTaper, and ProFile systems: breakage and distortion in severely curved roots of molars. *J Endod* 2004; 30: 234–237.
4. Iqbal MK, Kohli MR and Kim JS. A retrospective clinical study of incidence of root canal instrument separation in an endodontics graduate program: a PennEndo database study. *J Endod* 2006; 32: 1048–1052.
5. McGuigan MB, Louca C and Duncan HF. The impact of fractured endodontic instruments on treatment outcome. *Br Dent J* 2013; 214: 285–289.
6. Panitvisai P, Parunnit P, Sathorn C, et al. Impact of a retained instrument on treatment outcome: a systematic review and meta-analysis. *J Endod* 2010; 36: 775–780.
7. Wu J, Lei G, Yan M, et al. Instrument separation analysis of multi-used ProTaper Universal rotary system during root canal therapy. *J Endod* 2011; 37: 758–763.
8. Fu M, Zhang Z and Hou B. Removal of broken files from root canals by using ultrasonic techniques combined with dental microscope: a retrospective analysis of treatment outcome. *J Endod* 2011; 37: 619–622.
9. Shahabinejad H, Ghassemi A, Pishbin L, et al. Success of ultrasonic technique in removing fractured rotary nickel-titanium endodontic instruments from root canals and its effect on the required force for root fracture. *J Endod* 2013; 39: 824–828.
10. Ruddle CJ. Micro-endodontic nonsurgical retreatment. *Dent Clin North Am* 1997; 41: 429–454.
11. Wu Y, Cathro P and Marino V. Fracture resistance and pattern of the upper premolars with obturated canals and restored endodontic occlusal access cavities. *J Biomed Res* 2010; 24: 474–478.
12. Eraslan O, Eraslan O, Eskitascioglu G, et al. Conservative restoration of severely damaged endodontically treated premolar teeth: a FEM study. *Clin Oral Investig* 2011; 15: 403–408.
13. Zhao Y, Wang W, Xin H, et al. The remodeling of alveolar bone supporting the mandibular first molar with different levels of periodontal attachment. *Med Biol Eng Comput* 2013; 51: 991–997.
14. Belli S, Eraslan O and Eskitascioglu G. Effect of root filling on stress distribution in premolars with endodontic-periodontal lesion: a finite elemental analysis study. *J Endod* 2016; 42: 150–155.
15. Bonessio N, Arias A, Lomiento G, et al. Effect of root canal treatment procedures with a novel rotary nickel titanium instrument (TRUShape) on stress in mandibular molars: a comparative finite element analysis. *Odontology* 2017; 105: 54–61.
16. Dejak B and Mlotkowski A. 3D-Finite element analysis of molars restored with endocrowns and posts during masticatory simulation. *Dent Mater* 2013; 29: e309–e317.

17. Yuan K, Niu C, Xie Q, et al. Apical stress distribution under vertical compaction of gutta-percha and occlusal loads in canals with varying apical sizes: a three-dimensional finite element analysis. *Int Endod J* 2018; 51: 233–239.
18. Yoon HG, Oh HK, Lee DY, et al. 3-D finite element analysis of the effects of post location and loading location on stress distribution in root canals of the mandibular 1st molar. *J Appl Oral Sci* 2018; 26: e20160406.
19. Celik Koycu B, Imirzalioglu P and Ozden UA. Three-dimensional finite element analysis of stress distribution in inlay-restored mandibular first molar under simultaneous thermomechanical loads. *Dent Mater J* 2016; 35: 180–186.
20. Ward JR, Parashos P and Messer HH. Evaluation of an ultrasonic technique to remove fractured rotary nickel-titanium endodontic instruments from root canals: clinical cases. *J Endod* 2003; 29: 764–767.
21. Chang E, Lam E, Shah P, et al. Cone-beam computed tomography for detecting vertical root fractures in endodontically treated teeth: a systematic review. *J Endod* 2016; 42: 177–185.
22. Chen G, Fan W, Mishra S, et al. Tooth fracture risk analysis based on a new finite element dental structure models using micro-CT data. *Comput Biol Med* 2012; 42: 957–963.
23. Tang W, Wu Y and Smales RJ. Identifying and reducing risks for potential fractures in endodontically treated teeth. *J Endod* 2010; 36: 609–617.
24. Dane A, Capar ID, Arslan H, et al. Effect of different torque settings on crack formation in root dentin. *J Endod* 2016; 42: 304–306.
25. Brito-Junior M, Santos LA, Faria-e-Silva AL, et al. Ex vivo evaluation of artifacts mimicking fracture lines on cone-beam computed tomography produced by different root canal sealers. *Int Endod J* 2014; 47: 26–31.
26. Rosen E, Taschieri S, Del Fabbro M, et al. The diagnostic efficacy of cone-beam computed tomography in endodontics: a systematic review and analysis by a hierarchical model of efficacy. *J Endod* 2015; 41: 1008–1014.
27. Magne P. Efficient 3D finite element analysis of dental restorative procedures using micro-CT data. *Dent Mater* 2007; 23: 539–548.